View metadata, citation and similar papers at core.ac.uk

brought to you by CORE

provided by ScholarWorks@UNIST

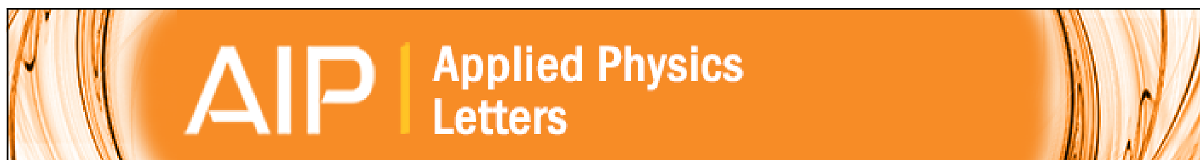

Observation of oxide precipitates in InN nanostructures

Soon-Yong Kwon, Zaiyuan Ren, Qian Sun, Jung Han, Young-Woon Kim, Euijoon Yoon, Bo Hyun Kong, Hyung Koun Cho, Il-Joong Kim, and Hyeonsik Cheong

Citation: Applied Physics Letters **91**, 234102 (2007); doi: 10.1063/1.2822396

View online: http://dx.doi.org/10.1063/1.2822396

View Table of Contents: http://scitation.aip.org/content/aip/journal/apl/91/23?ver=pdfcov

Published by the AIP Publishing

Articles you may be interested in

Selective-hydrogen sensing at room temperature with Pt-coated InN nanobelts
Appl. Phys. Lett. **93**, 202109 (2008); 10.1063/1.3033548

High-density InGaN nanodots grown on pretreated GaN surfaces
Appl. Phys. Lett. **89**, 023114 (2006); 10.1063/1.2218312

Near-red emission from site-controlled pyramidal InGaN quantum dots
Appl. Phys. Lett. **87**, 163121 (2005); 10.1063/1.2108126

InGaN nanorings and nanodots by selective area epitaxy
Appl. Phys. Lett. **87**, 143111 (2005); 10.1063/1.2056584

Characterization of oxide precipitates in epitaxial InN by transmission electron microscopy
Appl. Phys. Lett. **87**, 092102 (2005); 10.1063/1.2035330

is pleased to announce Reuben Collins as its new Editor-in-Chief

This article is copyrighted as indicated in the article. Reuse of AIP content is subject to the terms at: http://scitation.aip.org/termsconditions. Downloaded to IP: 114.70.7.203 On: Wed, 24 Sep 2014 06:23:30

APPLIED PHYSICS LETTERS **91**, 234102 (2007)

Observation of oxide precipitates in InN nanostructures

Soon-Yong Kwon,[a] Zaiyuan Ren, Qian Sun, and Jung Han
Department of Electrical Engineering, Yale University, New Haven, Connecticut 06520, USA

Young-Woon Kim and Euijoon Yoon
Department of Materials Science and Engineering, Seoul National University, Seoul 151-742, Korea

Bo Hyun Kong and Hyung Koun Cho
School of Advanced Materials Science and Engineering, Sungkyunkwan University, Suwon 440-746, Korea

Il-Joong Kim and Hyeonsik Cheong
Department of Physics, Sogang University, Seoul 121-742, Korea

(Received 31 August 2007; accepted 16 November 2007; published online 5 December 2007)

We observed the formation of oxide precipitates (bcc-In_2O_3) in InN nanostructures formed during metal-organic chemical vapor deposition (MOCVD) and/or subsequent postgrowth procedures in H_2 ambient. It was found that InN is extremely unstable in H_2 ambient and the activation energy of N_2 desorption of InN is measured to be ~0.28 eV, which is one order of magnitude smaller than that of reported value of InN in vacuum. Instability of InN nanostructures under H_2 ambient together with residual oxidant in the reactor facilitates the formation of indium oxide precipitates in the nanostructure matrix during MOCVD or the oxidation of residual indium at the surface, resulting in indium oxide dots. © *2007 American Institute of Physics*. [DOI: 10.1063/1.2822396]

Indium nitride (InN) has attracted much attention recently as an important group III-nitride semiconductor.[1] Although thermal instability of InN as well as large lattice and thermal mismatches make the growth of InN films extremely difficult,[1] recent results on InN-based nanostructures[2–4] are very promising and indicative of potential device applications. However, depending on the growth conditions, there is a possibility of oxide precipitation in such InN nanostructures during growth and/or postgrowth procedures because of high volatility of N_2 from InN surface[1,2] and high tendency for indium residue on surface to react with background molecular oxygen.[5] It is expected that oxidation would easily occur for indium residue on surface in preference to nitridation by considering the large difference in the heat of formation of InN (34 kcal/mol),[6] compared with In_2O_3 (221 kcal/mol).[5] Generally, InN is grown with N_2 carrier gas or a mixed carrier gas of N_2 and H_2 in metal-organic chemical vapor deposition (MOCVD) because of expected thermal instability of InN under H_2 ambient.[7] Up to date, there are a few empirical information on this specificity in the growth of InGaN;[8,9] however, the role of hydrogen is unclear and speculative in these reports. Therefore, it is desirable to investigate the role of hydrogen in detail in MOCVD growth of InN because hydrogen and hydrogen-containing derivatives are present during InN growth and it will provide a deeper understanding of the underlying chemistry. In this letter, we report the observation of oxide precipitates (bcc-In_2O_3) in InN nanostructures formed during MOCVD and/or postgrowth procedures in H_2 ambient. InN was extremely unstable in H_2 ambient and the appearance of oxide precipitates was very similar to that expected from genuine InN nanostructures, rendering a possibility of false detection.

Two sets of InN nanostructures were grown in commercial horizontal MOCVD reactors. Trimethylgallium, trimethylindium (TMIn), and ammonia (NH_3) were used as Ga, In, and N sources, respectively, whereas both high-purity H_2 and N_2 of 6*N* (99.9999%) were used as carrier gases. Hydrogen was further purified by a Pd purifier. The first set of InN nanostructures was grown on top of 20-nm-thick cubic GaN (*c*-GaN)/GaP(100) templates grown at 520 °C in H_2 ambient. The InN dots were grown at growth temperatures in the range of 450–550 °C and the growth pressure was 200 mbar. H_2 carrier gas (7.0 SLM) was introduced throughout the InN growth with NH_3 (3.75 SLM), where SLM stands for standard liters per minute. Immediately after the InN growth, H_2 carrier gas was replaced with N_2 and both N_2 carrier gas (7.0 SLM) and NH_3 (3.75 SLM) were introduced during cooling process to room temperature (RT). The growth rate of InN dots was controlled by TMIn flow rate. The TMIn flow rates were 7.5 and 15 μmol/min, and the corresponding growth times were 45 and 22.5 min, respectively, to keep the total amount of deposition from the gas-phase sources constant in all InN growth at a certain growth temperature. The second set of InN nanostructures is a few monolayer (ML)-thick InN epitaxial layers grown on 2-μm-thick GaN/sapphire(0001) templates. The growth of InN was performed at 730 °C for 90 s and the growth pressure was 300 Torr. All growth conditions were fixed, and TMIn (10 μmol/min) and NH_3 (4.0 SLM) were supplied as precursors and N_2 carrier gas (3.6 SLM) was used. After the InN growth, we varied the cooling environment, one is to keep flowing N_2 carrier gas (3.6 SLM) and NH_3 (4.0 SLM), while the samples was cooled down to RT, and the other is to keep flowing N_2 carrier gas and NH_3 down to 400 °C, followed H_2 carrier gas (7.6 SLM) down to RT.

Figure 1(a) shows a cross-section transmission electron microscope (TEM) image taken for InN dots grown on a *c*-GaN/GaP(100) template at 450 °C with TMIn flow rate of 15 μmol/min. The indexing of the diffraction pattern (DP) taken from overall structures (not shown here) proved that InN dots grow in zinc-blende structure, where *c*-InN(100)

[a]Author to whom correspondence should be addressed. Electronic mail: syong.kwon@gmail.com.

This article is copyrighted as indicated in the article. Reuse of AIP content is subject to the terms at: http://scitation.aip.org/termsconditions. Downloaded to IP: 114.70.7.203 On: Wed, 24 Sep 2014 06:23:30

 © 2007 American Institute of Physics

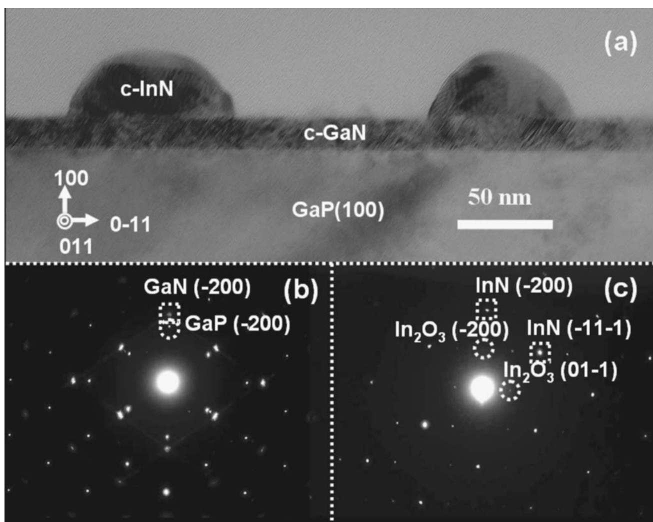

FIG. 1. (a) Cross-section TEM image of InN dots grown at 450 °C with TMIn flow rate of 15 μmol/min on 20-nm-thick c-GaN/GaP(100), (b) SADP of the interface between c-GaN buffer (square) and GaP(100) substrate (circle), and (c) SADP of the InN dot (square) with coexisting precipitates bcc-In_2O_3 (circle).

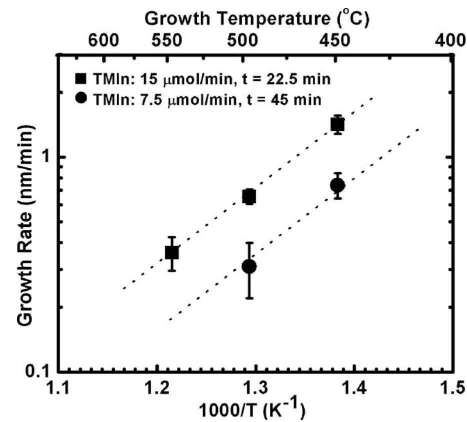

FIG. 2. Arrhenius plot of N_2 desorption-controlled growth rate of InN dots vs. substrate temperature at a constant amount of deposition from the gas-phase sources.

planes are parallel to c-GaN(100) planes and hexagonal InN is not present. However, an additional set of diffraction spots was found in this sample. We obtained selective area DPs (SADPs) to determine where they were originated and the additional set of diffraction spots was found only from InN dots, as shown in Figs. 1(b) and 1(c). Based on the corresponding angles and distances between the spots, the coexisting precipitates in InN dots were determined as body centered cubic (bcc)-In_2O_3. The oxide precipitates were uniformly distributed from the central to the edge area of InN dots from SADP, and it is reasonable to assume that the oxidation process occurred during MOCVD rather than post-growth process. We supposed that this phenomenon is related to low thermal stability of InN in H_2 ambient since hydrogen tends to etch InN and reduces nitrogen sticking coefficient in In(Ga)N, as predicted by thermodynamic calculations.[7]

This hypothesis was tested by growing InN dots with H_2 carrier gas on c-GaN/GaP(100) templates at a constant amount of deposition from the gas-phase sources but at different temperatures and growth rates. Growth temperatures were varied from 450 to 550 °C and the calculation of growth rate of InN dots was based on the assumption that the shape of InN dots was a perfect hemisphere. The results are shown in Fig. 2. Higher growth temperature leads to lower growth rate, indicating the strong thermal decomposition of InN during growth, and the activation energy is measured to be ~0.28 eV on the Arrhenius plot. This value is one order of magnitude smaller than the reported activation energy of N_2 desorption of InN (or GaN) in vacuum.[10,11] Based on this result, we concluded that the introduction of H_2 into the reactor greatly lowered the thermal stability of InN, which enhances the possibility of oxidation of InN.

We also find that surface oxidation of preexisting InN can occur depending on how growth was terminated. A few ML-thick InN was grown on 2-μm-thick GaN/sapphire(0001) template with typical step-flow like feature of atomically flat surface to see the surface morphology of the bare InN layer. After 90 s InN deposition, the sample was cooled down to RT with both N_2 and NH_3 flows and the resulting sample surface showed the stepped two-dimensional (2D) morphology with the formation of 2D disk-shaped structures on terraces, as shown in Fig. 3(a). Heights of 2D disk-shaped structures were about 3–5 Å as measured by atomic force microscopy (AFM), which are equivalent to 1–2 ML of InN and their diameters were less than 200 nm.[12] However, when N_2 carrier gas and NH_3 were switched off at 400 °C and the InN specimen was cooled down to RT under H_2 ambient, the surface morphology of InN was greatly changed. The quantum dot (QD)-like structures with a density of 2.5×10^9 cm^{-2} surprisingly appeared on InN surface and most of them existed on 2D disk-shaped structure from AFM measurement, as shown in Fig. 3(b).

From the cross-section TEM images, as shown in Fig. 4, the QD-like structures on InN surface have a different lattice image from underlying GaN template and it turns out to be bcc-In_2O_3 instead of InN. The interplanar spacing of high resolution lattice fringe image of In_2O_3 was ~2.9 Å and this corresponds to the reported lattice constant of bcc-In_2O_3(222),[13] which is in good agreement with a preferential orientation of In_2O_3 formed by thermal oxidation of InN.[14] We believe that decomposition and desorption of N_2 from InN surface were greatly enhanced under H_2 ambient during cooling process and the indium residue on the surface would strongly chemisorb background molecular oxygen,[5] resulting in bcc-In_2O_3 formation mainly on 2D disk-shaped structures.

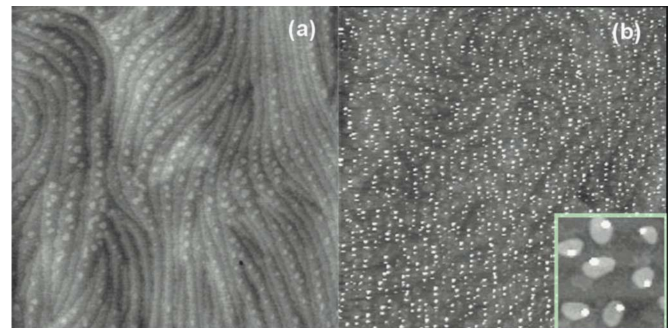

FIG. 3. (Color online) 4×4 μm^2 AFM images of a few ML-thick InN layers on GaN templates with a cooling environment of (a) N_2 carrier gas and NH_3 to RT and (b) N_2 carrier gas and NH_3 down to 400 °C, followed by only H_2 carrier gas down to RT. The inset depicts the formation of QD-like structures mostly on 2D disk-shaped structures.

This article is copyrighted as indicated in the article. Reuse of AIP content is subject to the terms at: http://scitation.aip.org/termsconditions. Downloaded to IP: 114.70.7.203 On: Wed, 24 Sep 2014 06:23:30

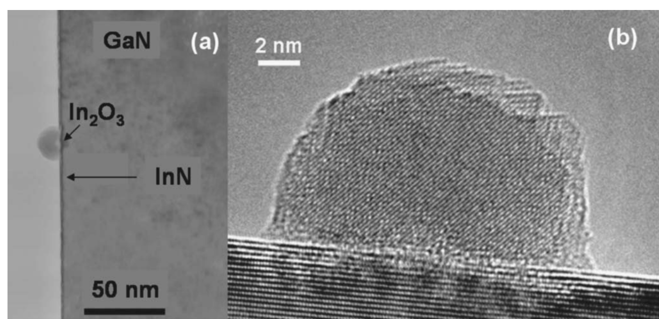

FIG. 4. (a) Cross-section TEM image of bcc-In_2O_3 formed on InN layer and (b) high resolution image of (a).

It is noteworthy that the oxidation of InN during MOCVD growth and/or subsequent postgrowth procedures would be a problem that must be taken into account during InN-based device fabrication. By considering the heats of formation of InN (34 kcal/mol) (Ref. 6) and In_2O_3 (221 kcal/mol),[5] the very small amount of background oxygen or water vapor existing in the reactor can lead to the detectable oxidation of InN. Even if InN growth is performed in an inert gas environment such as N_2, there is still a possibility of oxidation of InN since the hydrogen-containing derivatives from the decomposition of NH_3 (Ref. 7) and/or H_2 carrier gas introduced for the subsequent (Al)GaN growth can influence the thermal stability of preexisting InN nanostructures. We finally note that, as the size of InN is getting smaller, the possibility of false detection of oxide precipitates as InN dots, when an inappropriate ambient was provided, is getting larger by nominal characterization tools because of their structural similarity.

In conclusion, it was found that InN nanostructures are extremely sensitive to growth environment. InN is very unstable especially in H_2 ambient and the activation energy of N_2 desorption from InN in hydrogen ambient is measured to be $\sim$0.28 eV. The appearance of oxide precipitates was very similar to that expected from genuine InN nanostructures.

This work was supported by the DOE-NEFL Project. The work at Sogang was supported in part by the MOST/KOSEF through the Quantum Photonic Science Research Center. S.Y.K. acknowledges the support of the Korea Research Foundation Grant funded by Korea Government (MOEHRD, Basic Research Promotion Fund) (No. KRF-2005-214-D00315). E.Y. acknowledges the support from Center for Materials and Processes of Self-Assembly through MOST/KOSEF (No. R11-2005-048-00000-0).

[1] A. G. Bhuiyan, A. Hashimoto, and A. Yamamoto, J. Appl. Phys. **94**, 2779 (2003).
[2] S.-Y. Kwon, H. J. Kim, H. Na, Y.-W. Kim, H.-C. Seo, H. J. Kim, Y. Shin, E. Yoon, and Y.-S. Park, J. Appl. Phys. **99**, 044906 (2006).
[3] A. Yoshikawa, N. Hashimoto, N. Kikukawa, S. B. Che, and Y. Ishitani, Appl. Phys. Lett. **86**, 153115 (2005).
[4] S. Ruffenach, B. Maleyre, O. Briot, and B. Gil, Phys. Status Solidi C **2**, 826 (2005).
[5] B. R. Natarajan, A. H. Eltoukhy, J. E. Greene, and T. L. Barr, Thin Solid Films **69**, 217 (1980).
[6] J. B. MacChesney, P. M. Bridenbaugh, and P. B. O'Connor, Mater. Res. Bull. **5**, 783 (1970).
[7] A. Koukitu, T. Taki, N. Takahasi, and H. Seki, J. Cryst. Growth **197**, 99 (1999).
[8] F. Scholz, V. Härle, F. Steuber, H. Bolay, A. Dörnen, B. Kaufmann, V. Syganow, and A. Hangleiter, J. Cryst. Growth **170**, 321 (1997).
[9] E. L. Piner, M. K. Behbehani, N. A. El-Masry, F. G. McIntosh, J. C. Roberts, K. S. Boutros, and S. M. Bedair, Appl. Phys. Lett. **70**, 461 (1997).
[10] D. D. Koleske, A. E. Wickenden, R. L. Henry, M. E. Twigg, J. C. Culbertson, and R. J. Gorman, Appl. Phys. Lett. **73**, 2018 (1998).
[11] O. Ambacher, M. S. Brandt, R. Dimitrov, T. Metzger, M. Stutzmann, R. A. Fischer, A. Miehr, A. Bergmaier, and G. Dollinger, J. Vac. Sci. Technol. B **14**, 3532 (1996).
[12] H. J. Kim, H. Na, S.-Y. Kwon, H.-C. Seo, H. J. Kim, Y. Shin, K.-H. Lee, Y.-W. Kim, S. Yoon, H. J. Oh, C. Sone, Y. Park, Y.-H. Cho, Y. Sun, and E. Yoon, Phys. Status Solidi C **0**, 2834 (2003).
[13] JCPDS Card No. 06-0416, 1998.
[14] S. Luo, W. Zhou, Z. Zhang, J. Shen, L. Liu, W. Ma, X. Zhao, D. Liu, L. Song, Y. Xiang, J. Zhou, S. Xie, and W. Chu, Appl. Phys. Lett. **89**, 093112 (2006).

This article is copyrighted as indicated in the article. Reuse of AIP content is subject to the terms at: http://scitation.aip.org/termsconditions. Downloaded to IP: 114.70.7.203 On: Wed, 24 Sep 2014 06:23:30